International Journal of Scientific Research and Engineering Development-– Volume 9 Issue 1, Jan-Feb 2026
Available at www.ijsred.com

RESEARCH ARTICLE OPEN ACCESS

Analysis of Rocks around Elmithnab Al-Qassim Region Kingdom of Saudi Arabia Using Laser Induced Breakdown Spectroscopy

Mubarak M. Ahmed
Department of Physics, College of Science, Qassim University, P. O. Box 931, Buridah 51931, KSA.
M.ELMAHAL@qu.edu.sa

----------**********----------

Abstract:
We present laser induced breakdown spectroscopic studies of variety of rock samples around Elmithnab Al-Qassim region Kingdom of Saudi Arabia. The samples were collected from East, West, and North about 15 km from city center. Nd:YAG laser (1064 nm) in conjunction with Spectrograph equipped with computer is used to record the LIBS data. The emission spectra of these samples have been recorded as functions of laser irradiance. The elemental composition and the relative abundance in each sample are found to be They differ from region to region. Quantities of Iron, Calcium, Copper, Silicon, Aluminum, Manganese, Lead. sulfur and Zinc are detected in these samples.
Although the distribution of elements in the samples is not uniform, sulfur and silicon were found in higher concentrations than other elements in the area.

Keywords: Laser-induced breakdown spectroscopy (LIBS), plasma, rocks.

----------**********----------

I. INTRODUCTION

Laser-induced breakdown spectroscopy (LIBS) is a type of atomic emission spectroscopy which uses a highly energetic laser pulse as the excitation source, and it is atomic spectroscopy technique used to measure the concentration of major and trace elements in solid, liquid, or air samples, or to record the chemical signature (fingerprint) of a material. [1, 2]. Each LIBS spectrum contains not only information about the concentrations of all naturally-occurring elements, but also some isotopic ratios and information about the atomic structure of the material [3,4]. LIBS is a spot analysis technique, with laser ablation craters on the order of 30 - 400 µm diameter, depending on the laser wavelength, power, properties of the material itself, and how well the laser couples to the material [5, 6].
Because LIBS is a spot analysis technique, it is possible to evaluate spatial changes in material composition and also to average shots taken from many different locations on the materials to obtain a bulk composition [7].
A high-power laser pulse is used as an energy source to cause ablation of atoms from the sample surface and formation of a short-lived, high-temperature plasma. Plasma temperatures are generally hotter than 10,000 K with sufficient energy to cause excitation of electrons in outer orbitals [8, 9]. As the plasma cools, the excited electrons decay to lower-energy orbitals, emitting photons with wavelengths inversely proportional to the energy difference between the excited and base orbitals. There are many possible excited states and thus many emitted wavelengths for each element [10].
LIBS spectroscopy can be produced from a variety of lasers but typically excimers or pulsed Nd:Yag lasers are used. The high intensity laser pulse interacting with the sample produces a plasma plume that evolves with time from the point of impact of the incident laser pulse [8]. The laser pulse usually lasts for 5 to 20ns.The emission from the plasma plume is collected and analyzed by the detection system. Typically, the emission is collected at some distance from the sample to reduce the significance of self-absorption effects or surface effects [2]. The plasma created breaks down all the sample's chemical bonds and ionizes many of the

constituent elements. The spectral emission occurs as a result of the subsequent relaxation of the constituent excited species [1, 10]. The spectrum that is observed in the first 100ns is dominated by continuous, intense, white-light radiation; consequently, no discrete lines can be observed. The plasma plume expands with time and the excited species relax further. After around 1μs from the incident laser pulse, discrete spectral lines originating from various ionic species start to become visible. The spectra below indicate how the spectral lines evolve over time. The exact timing and the spectral lines vary with the type of sample, the distance from the center of the plasma and the wavelength of the incident laser light, but typically the evolution of the plasma and the changes in its content occur on a microsecond timescale [5, 8].

II. EXPERIMENTAL WORK

Ten rock samples were collected from various locations northwest of Elmithnab, along the road connecting Elmithnab and Unayzah. The surfaces of the rock samples were cleaned, polished, and cut into 2 cm diameter discs before the experiment.

In this research, a Spectro Laser Target Elemental Analysis System device was used. This is a Laser-induced breakdown spectroscopy device (LIBS). The laser used is a Neodymium YAG with a wavelength of 1064 nm, and pulse duration of 7 ns, and a frequency of 15 Hz. The system is equipped with a CCD camera, and sample tray, and the device is also connected to a computer with software program for analysis and measurements.

The computer allows for the adjustment of the laser parameters and the specific laser pulse type. The analysis is also performed on the computer, and the results are displayed in tables.

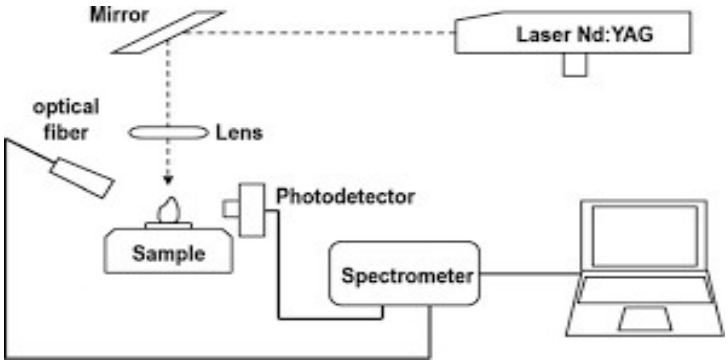

Fiure (1) Schematic diagram of LIBS system

III. RESULTS AND DISCUSSIONS

Tables 1 to 10 show the relative abundance of elements in the samples. Each table specifies the percentage concentration of each element relative to the total concentration of all measured components.

Table (1)

Sample 1	Concentration	relative abundance
S (Sulfur)	89.04	88.775%
Si (Silicon)	3.54	3.530%
Fe (Iron)	3.29	3.280%
Pb (Lead)	2.42	2.413%
Zn (Zinc)	1.41	1.406%
Ca (Calcium)	0.51	0.508%
Cu (Copper)	0.080	0.080%
Al (Aluminum)	0.007	0.007%
Mg (Magnesium)	0.001	0.001%

The analysis reveals that Sulfur (S) is the dominant element, accounting for nearly 88.78% of the sample. This extremely high sulfur content, combined with significant levels of Iron (Fe), Lead (Pb), and Zinc (Zn), suggests the sample is likely a sulfide-rich mineral (such as galena or sphalerite matrix). Silicon (Si) is the primary non-metallic impurity (3.53%). Elements like Magnesium (Mg) and Aluminum (Al) are present in trace amounts, indicating they are likely minor inclusions or surface contaminants rather than part of the primary mineral structure.

Table (2)

Sample 2	**Concentration**	**relative abundance**
S (Sulfur)	60.52	89.165%
Si (Silicon)	3.54	5.216%
Zn (Zinc)	1.41	2.077%
Fe (Iron)	1.35	1.989%
Pb (Lead)	0.92	1.355%
Cu (Copper)	0.08	0.118%
Ca (Calcium)	0.046	0.068%
Al (Aluminum)	0.007	0.010%
Mg (Magnesium)	0.001	0.001%

Sample 2 is heavily dominated by Sulfur (S), which constitutes approximately 89.17% of the total elemental composition. While the absolute concentration of sulfur is lower than in Sample 1, its relative abundance is higher, indicating a more concentrated sulfur matrix. Silicon (Si) is the secondary major component at 5.22%, likely representing silicate impurities. The presence of Zinc, Iron, and Lead in significant relative proportions suggests this sample is a polymetallic sulfide mineral. Aluminum, Calcium, and Magnesium remain at trace levels, suggesting they are negligible in the mineral's primary structure.

Table (3)

Sample 3	**Concentration**	**relative abundance**
S (Sulfur)	89.04	77.908%
Zn (Zinc)	15.87	13.886%
Si (Silicon)	3.54	3.097%
Fe (Iron)	3.22	2.817%
Pb (Lead)	2.38	2.082%
Ca (Calcium)	0.15	0.131%
Cu (Copper)	0.08	0.070%
Al (Aluminum)	0.007	0.006%
Mg (Magnesium)	0.001	0.001%

In Sample 3, Sulfur (S) remains the dominant element at 77.91%, but there is a significant shift compared to previous samples. The Relative Abundance of Zinc (Zn) has increased dramatically to 13.89%, indicating that this specific sample is likely a Sphalerite-rich (ZnS) mineral or a complex sulfide ore with high zinc mineralization. Silicon (Si) and Iron (Fe) represent the primary gangue or secondary metallic components. The trace levels of Aluminum and Magnesium confirm that the sample is almost entirely composed of heavy metallic sulfides rather than silicate rock.

Table (4)

Sample 4	Concentration	relative abundance
S (Sulfur)	89.04	68.252%
Zn (Zinc)	15.87	12.165%
Pb (Lead)	11.6	8.892%
Fe (Iron)	7.11	5.450%
Si (Silicon)	3.54	2.714%
Ca (Calcium)	1.92	1.472%
Cu (Copper)	1.37	1.050%
Al (Aluminum)	0.007	0.005%
Mg (Magnesium)	0.001	0.001%

Sample 4 demonstrates a shift toward a complex polymetallic composition. While Sulfur (S) remains the primary component at 68.25%, its relative dominance is lower than in previous samples due to the significant rise in base metals. Zinc (12.17%), Lead (8.89%), and Iron (5.45%) are present in substantial proportions, suggesting the sample is likely a concentrated sulfide ore (possibly a mixture of sphalerite, galena, and pyrite). Additionally, the increase in Copper (1.05%) and Calcium (1.47%) indicates a more heterogeneous mineral matrix compared to the earlier, more "pure" sulfur samples.

Table (5)

Sample 5	Concentration	relative abundance
S (Sulfur)	89.04	68.252%
Zn (Zinc)	15.87	12.165%
Pb (Lead)	11.6	8.892%
Fe (Iron)	7.11	5.450%
Si (Silicon)	3.54	2.714%
Ca (Calcium)	1.92	1.472%
Cu (Copper)	1.37	1.050%
Al (Aluminum)	0.007	0.005%
Mg (Magnesium)	0.001	0.001%

Sample 5 (identical in composition to Sample 4) represents a highly polymetallic sulfide matrix. While Sulfur (S) remains the primary constituent at 68.25%, the sample is characterized by a high metallic diversity. The significant presence of Zinc (12.17%), Lead (8.89%), and Iron (5.45%) indicates a complex ore, likely a mixture of Sphalerite (ZnS), Galena (PbS), and Pyrite (FeS_2). The minor amounts of Calcium and Copper further suggest a more complex hydrothermal origin compared to simpler sulfur-rich samples.

Table (6)

Sample 6	Concentration	relative abundance
S (Sulfur)	89.04	76.853%
Zn (Zinc)	15.87	13.698%
Pb (Lead)	3.95	3.409%
Si (Silicon)	3.54	3.055%
Fe (Iron)	2.91	2.512%
Ca (Calcium)	0.46	0.397%
Cu (Copper)	0.08	0.069%
Al (Aluminum)	0.007	0.006%
Mg (Magnesium)	0.001	0.001%

Sample 6 is primarily composed of Sulfur (76.85%), followed by a significant Zinc (13.70%) component. This profile suggests a sulfide-based mineral, likely dominated by Sphalerite (ZnS) with secondary amounts of Galena (PbS) and Pyrite (FeS_2). Compared to Sample 5, this sample shows a lower lead-to-zinc ratio and a reduction in calcium, indicating a different mineralogical grade or a more pure zinc-sulfide deposit. Silicon remains the primary non-metallic impurity, likely originating from quartz or silicate gangue.

Table (7)

Sample 7	Concentration	relative abundance
S (Sulfur)	89.04	91.498%
Si (Silicon)	3.54	3.638%
Fe (Iron)	2.20	2.261%
Zn (Zinc)	1.41	1.449%
Pb (Lead)	0.97	0.997%
Cu (Copper)	0.08	0.082%
Ca (Calcium)	0.065	0.067%
Al (Aluminum)	0.007	0.007%
Mg (Magnesium)	0.001	0.001%

Sample 7 exhibits an extremely high concentration of Sulfur (91.50%), which is the highest relative abundance observed among the samples provided thus far. The presence of Silicon (3.64%) and Iron (2.26%) as the next most abundant elements suggests a mineral matrix primarily composed of native sulfur or a very high-grade sulfide deposit with minor silicate (quartz) and iron-sulfide (pyrite) impurities. Unlike Samples 4 and 5, the lower relative abundance of Lead and Zinc indicates a less complex polymetallic structure, pointing toward a more uniform sulfur-rich geochemical environment.

Table (8)

Sample 8	Concentration	relative abundance
S (Sulfur)	89.04	91.134%
Si (Silicon)	3.54	3.623%
Fe (Iron)	2.64	2.702%
Zn (Zinc)	1.41	1.443%
Pb (Lead)	0.92	0.942%
Cu (Copper)	0.08	0.082%
Ca (Calcium)	0.064	0.066%
Al (Aluminum)	0.007	0.007%
Mg (Magnesium)	0.001	0.001%

Sample 8 is characterized by an extreme dominance of Sulfur (91.13%), indicating a high-purity sulfur matrix. Silicon (3.62%) and Iron (2.70%) represent the primary secondary components, likely existing as quartz inclusions and iron-sulfide traces (pyrite). The metallic diversity (Zn, Pb, Cu) is relatively low compared to previous polymetallic samples, suggesting this specimen is closer to native sulfur or a simple monometallic sulfide ore. Trace elements such as Aluminum and Magnesium are nearly non-existent, further emphasizing the high purity of the sulfur-rich deposit.

Table (9)

Sample 9	Concentration	relative abundance
S (Sulfur)	69.14	89.129%
Si (Silicon)	3.54	4.564%
Fe (Iron)	2.41	3.107%
Zn (Zinc)	1.41	1.818%
Pb (Lead)	0.92	1.186%
Cu (Copper)	0.08	0.103%
Ca (Calcium)	0.064	0.083%
Al (Aluminum)	0.007	0.009%
Mg (Magnesium)	0.001	0.001%

Sample 9 is characterized by an overwhelming dominance of Sulfur (89.13%), which serves as the primary matrix. The presence of Silicon (4.56%) suggests minor silicate or quartz impurities. The metallic profile is dominated by Iron (3.11%), Zinc (1.82%), and Lead (1.19%), indicating that the sample is a polymetallic sulfide ore. Elements such as Aluminum, Calcium, and Magnesium appear only in trace amounts, suggesting that the sample is relatively free from common crustal rock contaminants.

Table (10)

Sample 10	Concentration	relative abundance
S (Sulfur)	89.04	84.632%
Fe (Iron)	7.11	6.758%
Si (Silicon)	3.54	3.365%
Ca (Calcium)	3.10	2.947%
Zn (Zinc)	1.41	1.340%
Pb (Lead)	0.92	0.874%
Cu (Copper)	0.08	0.076%
Al (Aluminum)	0.007	0.007%
Mg (Magnesium)	0.001	0.001%

Sample 10 presents a polymetallic sulfide profile with a notable enrichment in Iron (6.76%) and Calcium (2.95%) compared to Sample 9. While Sulfur still comprises the vast majority of the matrix (84.63%), the increased presence of Iron and Silicon suggests a higher proportion of pyrite (FeS2cap F e cap S sub 2 $FeS2$) and silicate gangue minerals. The metallic components—specifically Zinc and Lead—remain significant, indicating that this sample is part of a complex hydrothermal or sedimentary deposit. The negligible amounts of Aluminum and Magnesium suggest a clean mineral separation from common clay or crustal materials.

Below is the Comparative Summary Table of the Relative Abundance (%) for all 10 samples, followed by a mineralogical trend analysis.

Table (11)

Sample	S	Si	Fe	Zn	Pb	Ca	Cu	Al	Mg
S1	88.78	3.53	3.28	1.41	2.41	0.51	0.08	0.01	0.00
S2	89.17	5.22	1.99	2.08	1.36	0.07	0.12	0.01	0.00
S3	77.91	3.10	2.82	13.89	2.08	0.13	0.07	0.01	0.00
S4	68.25	2.71	5.45	12.17	8.89	1.47	1.05	0.01	0.00
S5	68.25	2.71	5.45	12.17	8.89	1.47	1.05	0.01	0.00
S6	76.85	3.06	2.51	13.70	3.41	0.40	0.07	0.01	0.00

S7	91.50	3.64	2.26	1.45	1.00	0.07	0.08	0.01	0.00
S8	91.13	3.62	2.70	1.44	0.94	0.07	0.08	0.01	0.00
S9	89.13	4.56	3.11	1.82	1.19	0.08	0.10	0.01	0.00
S10	84.63	3.37	6.76	1.34	0.87	2.95	0.08	0.01	0.00

Mineralogical Trend Analysis

1. Sulfide Matrix Dominance: Sulfur (S) remains the primary matrix across all samples. However, there is an inverse relationship between Sulfur and metal concentration; when metallic elements (Zn, Pb, Fe) increase (as seen in Samples 4 ,(5 & the relative sulfur percentage drops to its lowest levels (~68%).
2. Zinc-Lead Enrichment Zones: Samples 3, 4, 5, and 6 represent "Ore-Grade" zones. The high abundance of Zinc (up to 13.89%) and Lead (up to 8.89%) suggests a strong presence of minerals like Sphalerite (ZnS) and Galena (PbS).
3. High-Purity Sulfur Zones: Samples 7 and 8 represent the highest purity of Native Sulfur or monometallic sulfide, with sulfur abundance exceeding .%91 These samples have the lowest levels of heavy metal impurities.
4. Iron and Gangue Variations: Silicon (Si) is consistently present (2.7% – 5.2%), indicating a persistent quartz/silicate gangue. Sample 10 shows a unique spike in Calcium (2.95%) and Iron (6.76%) , possibly indicating a transition into a Pyrite (FeS_2) or Calcite-rich mineral vein.

IV. CONCLUSION

Elemental composition analysis of rocks in the area northwest of Al-Muthnib, Al-Qassim, Saudi Arabia, using LIBS laser spectroscopy, revealed the presence of iron, calcium, carbon, silicon, aluminum, copper, magnesium, lead, and zinc in the surface rocks of the region.

Although the distribution of elements in the samples is not uniform, sulfur and silicon were found in higher concentrations than other elements in the area.

In the near future, we intend to conduct further elemental composition studies of rocks in other areas of the Al-Qassim region, as well as studies of rocks at various depths below the Earth's surface.

REFERENCES

[1] Cremers, D. A., & Knight, L. J. (2013). *Handbook of Laser-Induced Breakdown Spectroscopy*. John Wiley & Sons.

[2] Miziolek, A. W., Palleschi, V., & Schechter, I. (2006). *Laser-Induced Breakdown Spectroscopy (LIBS): Fundamentals and Applications*. Cambridge University Press.

[3] Harmon, R. S., Russo, R. E., & Hark, R. R. (2013). Applications of laser-induced breakdown spectroscopy for geochemical and environmental analysis: A review. *Spectrochimica Acta Part B: Atomic Spectroscopy*, 87, 11-26.

[4] Singh, J. P., & Thakur, S. N. (2020). *Laser-Induced Breakdown Spectroscopy*. (2nd Ed.). Elsevier.

[5] Noll, R. (2012). *Laser-Induced Breakdown Spectroscopy: Fundamentals and Applications*. Springer Science & Business Media.

[6] Senesi, G. S., & Harmon, R. S. (2023). Laser-induced breakdown spectroscopy (LIBS) for geological and environmental applications: A review. *Journal of Geochemical Exploration*, 244, 107113.

[7] Yuan, T., Wang, Z., Ni, J., & Liu, J. (2021). Machine learning in laser-induced breakdown spectroscopy: A review. *Analytica Chimica Acta*, 1184, 338802.

[8] Hahn, D. W., & Omenetto, N. (2012). Laser-induced breakdown spectroscopy (LIBS), part I: Review of basic diagnostics and plasma-particle interactions. *Applied Spectroscopy*, 66(4), 347-419.

[9] Tognoni, E., Palleschi, V., Corsi, M., & Cristoforetti, G. (2002). Quantitative micro-analysis by laser-induced breakdown spectroscopy: A review of the results. *Spectrochimica Acta Part B: Atomic Spectroscopy*, 57(7), 1115-1130.

[10] Musazzi, S., & Perini, U. (2014). *Laser-Induced Breakdown Spectroscopy: Theory and Applications*. Springer.

